Proceedings of the 3rd IASME/WSEAS Int. Conf. on HEAT TRANSFER, THERMAL ENGINEERING AND ENVIRONMENT, Corfu, Greece, August 20-22, 2005 (pp366-372)

Numerical Assessment of the Allowed Sulphur Content in the Fuel Used by the Power Stations in Kuwait – Part 2

A.A. RAMADAN†, M. AL-SUDAIRAWI, S. AL-HAJRAF AND A. KHAN

† Corresponding author
Coastal and Air Pollution Department
Environment and Urban Development Division
Kuwait Institute for Scientific Research
P.O. Box 24885, 13109 Safat – Kuwait
aramadan@kisr.edu.kw
http://www.kisr.edu.kw

Abstract:- In this communication we present results obtained using the Industrial Sources Complex Short Term (ISCST3) model to calculate the SO_2 concentration resulting from existing power stations in Kuwait assuming a) zero background SO_2 concentration and b) entire reliance on Heavy Fuel Oil (HFO). Different scenarios represented by different fuel sulphur content (S%) were simulated. Part 1 reports on the model used, assumptions made, scenarios considered and results for CASE 1. This part discusses the results for CASES 2, 3 and 4. The results reported here and in the accompanying Part 1 demonstrate that for the existing power stations in Kuwait, the annual SO_2 concentrations for fuels with low sulphur content do not pose any risk on urban populations. Bubyan Island and Subiya are considered ideal locations for future power stations. The majority of the pollutants around Kuwait City results from emissions from Doha East and Doha West power stations. The results are expected to benefit Kuwait Petroleum Corporation in improving the quality of the fuel produced for consumption by the power stations in Kuwait in order to maintain an acceptable ground level of SO_2.

Key-Words:- Sulphur Dioxide, Air Pollution, Air Quality, ISCST3 Model

1 Introduction

In the last century, advancement in industrialisation and medical care has increased the population, their life expectancy and also elevated their living standards. This development have resulted into unbearable constrain on the environment. Sulphur dioxide (SO_2) and nitrogen oxides (NO_x) emissions from power plants are just two examples of the results of the mentioned development. These two pollutants undergo changes in two forms: a) chemical change into sulphuric and nitric acids in the atmosphere through hydroxyl ion (OH^-) or ozone (O_3) oxidation in the gaseous phase and later deposition or b) transfer directly into the aqueous phase by rain. A considerable damage has resulted to the ecosystems where soil and buildings lacked the alkalinity to buffer the acid rain.

To assess and control the damage resulting from air pollutants, researchers have resorted to plume or puff dispersion numerical models. The application of plume/puff models is subjected to the use of results, either for risk assessment or for criteria pollutant analysis where peak value is only required irrespective of time and space. The most common plume dispersion models, e.g. ISCST3, have limitations: a) based on straight-line steady state flow fields, b) applicable within limited distances (e.g. 50km in the case of ISCST3) and, c) can be used for single pollutant only. On the other hand, comprehensive dispersion models, e.g. CALPUFF, have the following advantages: a) can be applied for long range transport, b) can perform calculations for multiple pollutants at the same time and c) they cope with complex flow conditions including temporal and spatial variation in flow fields due to complex terrain, non-uniform land use patterns, coastal effects, etc. In this communication we present the results obtained using ISCST3. Calpuff results are expected to be the subject of future communications.

[1] have compared ISCST3 and CALPUFF models for several fumigated fields serving as source of (CH_3Br) in Salinas Valley, California. The simulated results have been compared with field measurements from 11 sites on adjacent mountains, valley floor and at Pacific Ocean coast over a 4 days period. With the lower of the two estimates, ISCST3 model underpredicted concentrations for 76% of data and averaged 66% of measured, and the CALPUFF model also underpredicted 67% of

observations and averaged 84% of measured. With the higher of the two estimates, ISCST3 overpredicted concentrations by a factor of 2 for 67% of data and CALPUFF overpredicted concentrations by a factor of 1.6 for over 50% of data.

2 Results and Discussion

Similar to Part 1, the isopleths plots presented show regions of SO_2 concentrations above KEPA threshold for residential areas. The hourly data plots are not shown due to space restrictions.

2.1 CASE 2: Subiya Power Station

2.1.1 Hourly

The hourly SO_2 concentrations due to S station are above the KEPA hourly threshold value even at the lowest S%. The region of high concentration is rather large. Amongst the areas affected are Kuwait Bay, Kuwait City, Salmiya City and Failaka Island. At 4S%, most of the areas mentioned suffer from SO_2 concentration above 2000μg/m^3 nearly four times the KEPA hourly threshold value. The point of highest concentration is at 1.6km from the station at an angle of 115^o (southwest).

2.1.2 Daily

As Figs. 1 show, the SO_2 concentrations are less noticeable for the daily isopleths plots for the lower S% and the effect is limited to the offshore region. At S% increases beyond 1S%, the western part of Failaka Island and the beach around Salmiya City start to become affected by SO_2 concentrations in excess of the KEPA daily standards and for 4S%, the whole calculation region is affected by high SO_2 concentrations. The point of maximum SO_2 concentration is closer to the station (at 1.4km) compared to the hourly case but still offshore. The effect of the prevailing north-western wind direction is more obvious as this point is at an angle of 169^o from the station (southwest). The maximum daily concentrations are listed in Table 1.

2.1.3 Annual

Figs. 2 show that the SO_2 annual concentrations remain less than the KEPA annual value until S% surpasses 1S%. The location of this station seems to be ideal as the region of high SO_2 annual concentration remains offshore even for the highest S% content of 4S%. Similar to the case of ZS station, the effect of the north-western prevailing wind direct is quite evident here. The point of highest concentration is in the middle of the Gulf at 4km from the station at an angle of 208^o (southeast). The maximum daily concentrations and their locations are listed in Table 2.

2.2 CASE 3: Doha East And Doha West Power Stations

2.2.1 Hourly

Due to the combined effect of the two stations, the hourly SO_2 concentrations for lowest S% exceed the KEPA hourly limit. A quick comparison with ZS and S reveals that for the lower S% the SO_2 hourly concentration was not as high as for this case. The high SO_2 concentrations cover Kuwait Bay as well as other nearby urban areas. The maximum SO_2 hourly concentration occurs at a point which is 1.7km at an angle = 113^o southwest of the stations. Whilst this point is at the similar distance and angle as the case for ZS and S stations, the effect of the sea and land breezes is quite apparent in the increased levels of SO_2 concentrations in the western-eastern direction. This phenomenon is cancelled out when the daily and annual averages are calculated as is seen in Figs. 3 and 4.

2.2.2 Daily

Similar to the hourly concentrations, the daily SO_2 concentrations exceed the KEPA limits for the lowest S% content as seen in Figs. 3. Due to the combined effect of the two stations, the region of high SO_2 concentration for the same S% is larger compared with the cases for ZS and S. As S% exceeds 1S%, the high SO_2 concentration covers most of the computational domain including Kuwait Bay and nearby cities. The maximum daily concentration occurs at 2.5km from the stations to the north-western direction (angle = 31.8^o). At 4S% the minimum SO_2 concentration is well above 157μg/m^3. Table 3 lists the maximum SO_2 concentrations and their locations relative to the centroid of the two stations.

2.2.3 Annual

Figs. 4 show that at 1S%, the SO_2 concentration exceeds the KEPA annual threshold over a small area near Sulaibikhat City. Similar to the remark made for the hourly and daily concentrations, the combined effect of the two stations is obvious in the high SO_2 concentrations even for smaller S%. As S% in the fuel increases, the region suffering from high SO_2 concentration widens and stretches in the south-eastern direction following the prevailing wind direction. Beyond 1S%, the high

concentration region starts to border urban areas like Andalus City. At 2S%, a completely detached low concentration region appears to the north-western side of the stations. This region grows as S% increases and at 4S% it joins the main plume and starts affecting Al-Jahra City. The authors are unable to explain this phenomenon although it is in agreement with the location of the maximum hourly SO_2 concentration observed above. Table 4 shows that the maximum concentration point for the annual case is always at 4.1km from the stations at 208^o angle (southeast).

2.3 CASE 4: Doha East And Doha West Power Stations-Optimised Grid Location

Having run the model with DE and DW at the centre of the grid it was decided to re-run the model but with the grid moved so the two stations are on the upper left corner of the grid. By comparing the results of this case to the standard one, it is expected to shed some light on the accuracy of the model's calculations in situations similar to this. Due to the strong prevailing wind direction, this tactic, if used with cautious, can help the researchers extend their region of prediction by about 25km in the prevailing wind direction.

2.3.1 Hourly

The results here are similar to what was seen in the standard case (CASE 3 above), but they have the advantage of showing the SO_2 concentrations over more cities to the southeast of the stations considered. The maximum SO_2 concentration occurs at the same locations as in CASE 3, i.e. 1.7km at an angle = 113^o southwest of the stations. The effect of sea and land breezes is less obvious here due to grid location to the eastern side of the stations. However, it is expected to continue to be dominant.

2.3.2 Daily

Observing Figs. 5 leads to the same remark as was made on the hourly concentrations in section 2.3.1 above due to the optimised grid location. The cumulative effect of the two stations is noticeable, i.e. the region of high SO_2 concentration for the same S% is larger compared with the cases for ZS and S. Contrary to the hourly concentrations results, the maximum daily concentration occurs at a different location than in CASE 3. For the optimised grid, the maximum SO_2 concentration is at 1.4km from the stations nearly to the south (angle = 176^o). The reason for what seems to be a peculiar phenomenon is very simple. The new grid does not cover the location of the maximum SO_2 concentration that was found in CASE 3, hence the point at 1.4km from the stations represent the second maximum SO_2 concentration. Table 5 lists the maximum SO_2 concentrations and their locations relative to the centroid of DE and DW.

2.3.3 Annual

As can be seen in Figs. 6, the advantage of the optimised grid location is not obvious for the lower S% when the plume is nearly contained within the computational domain for CASES 3&4. This is due to the strong north-western prevailing wind direction. As S% increases above 1S%, the optimised grid covers larger region of the areas affected by the high SO_2 concentration. The combined effect of the two stations is obvious in the high SO_2 concentrations even for smaller S%. As S% in the fuel increases, the region suffering from high SO_2 concentration widens and stretches in the south-eastern direction following the prevailing wind direction. At 2S%, the detached low concentration region observed in CASE 3 appears and it grows as S% increases to join the main plume at 4S%. The optimised grid location does not cover Al-Jahra City, but it is expected that Al-Jahra will be affected by the high SO_2 concentration at 4S%. The location of the maximum SO_2 concentration continues to be to the south-east direction as in CASE 3 (at 4.5km at 211^o angle) as shown in Table 6.

3 Concluding Remarks

The locations of the existing power stations have many benefits, e.g. a) proximity to sea water which is used for desalination as well as for steam turbines and cooling purposes and b) due to the prevailing north-western wind direction the high pollutant concentrations for ZS and S power stations occur offshore. This is plausible when considering that serious pollution episodes in cities aren't directly caused by sudden increase in pollutant emissions but result from unfavourable meteorological conditions [2]. According to [2], the meteorological parameters that provoke pollutants increase are: temperature, relative humidity and wind. As can be seen from CASE 4, optimising the grid location has to be used with cautious as it can conceal the location of the highest concentrations.

The hourly (not shown here) and daily concentration plots were observed to involve large amount of scatter, with less scatter in the latter plots. Both plots are useful in assessing whether the

pollutant levels violate KEPA values or not. The annual concentration plots show plumes aligned with the north-western prevailing wind direction. ZS and S seem to have ideal locations as with the effect of the strong prevailing wind direction, most of the pollutants are driven towards the middle of the Arabian Gulf with minimal effect on urban areas. The proximity as well as the north-west location of DW and DE to urban areas cause these areas to be largely affected with pollutants emitted from these stations even at small S%. Bubyan Island or near Subiya seems to be the ideal location for future power stations. However, the increased airborne pollutant levels above the Arabian Gulf is expected to have adverse effect on the marine life. Until the time has come to completely switch to cleaner fuels and renewable sources of energy the best solutions seems to improve the efficiency of power generation systems through: a) Combined–cycle systems, b) Combined heat and power production, c) System rehabilitation and boiler tuning and d) Electric power system interconnections [3].

9 Future Work

- Predict SO_2 concentration in the future based on the expected increase in energy demand as supplied by the National Control Centre-Kuwait.
- Re-run the ISCST3 model with the season/hourly load cycle.
- Use long range model (CALPUFF) to study the cumulative effect of all power stations in Kuwait

References:

[1] Honaganahalli, P. S. and Seiber, J. N., 2000, Measured and predicted airshed concentrations of methyl bromide in an agricultural valley and applications to exposure assessment, Atmospheric Environment 34, 3511-3523.

[2] Alkama, R. and Ourtirane K. 2004. Statistical study of air pollution from mobile source emissions in the Bejaia city (Algeria). Proceedings, Dubai International Conference on Atmospheric Pollution. Feb. 2004.

[3] Hamzeh, Ali. 2004. Improving Air Quality by Reducing Emissions from Electric Power Industry. Case Study: Thermal Power Plants in Syria. Proceedings, Dubai International Conference on Atmospheric Pollution. Feb. 2004.

	S%	Max. 24Hr	LOCATION		Dist (km)	Angle	Dir
			Long	Lat			
1	0.50%	384	802665	3272897	1.4	169.13	SW
2	0.75%	576	802665	3272897	1.4	169.13	SW
3	1%	768	802665	3272897	1.4	169.13	SW
4	1.50%	1152	802665	3272897	1.4	169.13	SW
5	2%	1536	802665	3272897	1.4	169.13	SW
6	3%	2304.1	802665	3272897	1.4	169.13	SW
7	4%	3072.1	802665	3272897	1.4	169.13	SW

Table 1: Maximum daily SO_2 concentrations and their locations (Subiya)

	S%	Max. 1Yr	LOCATION		Dist (km)	Angle	Dir
			Long	Lat			
1	0.50%	44.1	804840	3270684	4.0	208.37	SE
2	0.75%	66.2	804840	3270684	4.0	208.37	SE
3	1%	88.2	804840	3270684	4.0	208.37	SE
4	1.50%	132.3	804840	3270684	4.0	208.37	SE
5	2%	176.4	804840	3270684	4.0	208.37	SE
6	3%	264.6	804840	3270684	4.0	208.37	SE
7	4%	352.8	804840	3270684	4.0	208.37	SE

Table 2: Maximum annual SO_2 concentrations and their locations (Subiya)

	S%	Max. 24Hr	LOCATION		Dist (km)	Angle	Dir
			Long	Lat			
1	0.50%	609.7	767591	3252028	2.5	31.80	NW
2	0.75%	914.6	767591	3252028	2.5	31.80	NW
3	1%	1219.5	767591	3252028	2.5	31.80	NW
4	1.50%	1829.2	767591	3252028	2.5	31.80	NW
5	2%	2438.9	767591	3252028	2.5	31.80	NW
6	3%	3658.4	767591	3252028	2.5	31.80	NW
7	4%	4877.8	767591	3252028	2.5	31.80	NW

Table 3: Maximum daily SO_2 concentrations and their locations (DE & DW)

	S%	Max. 1Yr	LOCATION		Dist (km)	Angle	Dir
			Long	Lat			
1	0.50%	95.7	771660	3247095	4.1	208.39	SE
2	0.75%	143.6	771660	3247095	4.1	208.39	SE
3	1%	191.5	771660	3247095	4.1	208.39	SE
4	1.50%	287.2	771660	3247095	4.1	208.39	SE
5	2%	383	771660	3247095	4.1	208.39	SE
6	3%	574.5	771660	3247095	4.1	208.39	SE
7	4%	765.9	771660	3247095	4.1	208.39	SE

Table 4: Maximum annual SO_2 concentrations and their locations (DE & DW)

	S%	Max. 24Hr	LOCATION		Dist (km)	Angle	Dir
			Long	Lat			
1	0.50%	610.3	769598	3249316	1.4	175.82	SW
2	0.75%	915.5	769598	3249316	1.4	175.82	SW
3	1%	1220.7	769598	3249316	1.4	175.82	SW
4	1.50%	1831	769598	3249316	1.4	175.82	SW
5	2%	2441.4	769598	3249316	1.4	175.82	SW
6	3%	3662.1	769598	3249316	1.4	175.82	SW
7	4%	4882.74	769598	3249316	1.4	175.82	SW

Table 5: Maximum daily SO_2 concentrations and their locations (DE & DW) - Optimised Grid Location

	S%	Max. 1Yr	LOCATION		Dist (km)	Angle	Dir
			Long	Lat			
1	0.50%	96.1	772059	3246855	4.5	211.39	SE
2	0.75%	144.1	772059	3246855	4.5	211.39	SE
3	1%	192.2	772059	3246855	4.5	211.39	SE
4	1.50%	288.2	772059	3246855	4.5	211.39	SE
5	2%	384.3	772059	3246855	4.5	211.39	SE
6	3%	576.5	772059	3246855	4.5	211.39	SE
7	4%	768.67	772059	3246855	4.5	211.39	SE

Table 6: Maximum annual SO_2 concentrations and their locations (DE & DW) - Optimised Grid Location

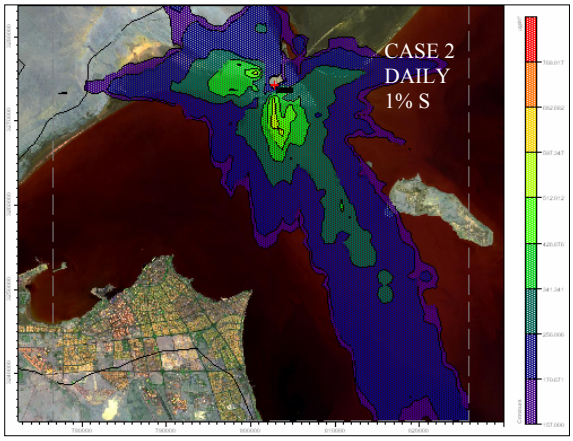

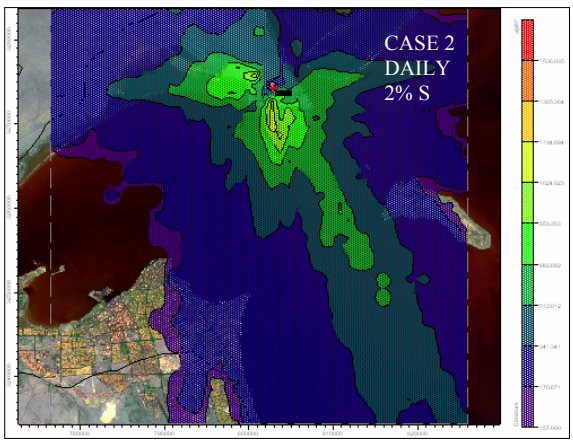

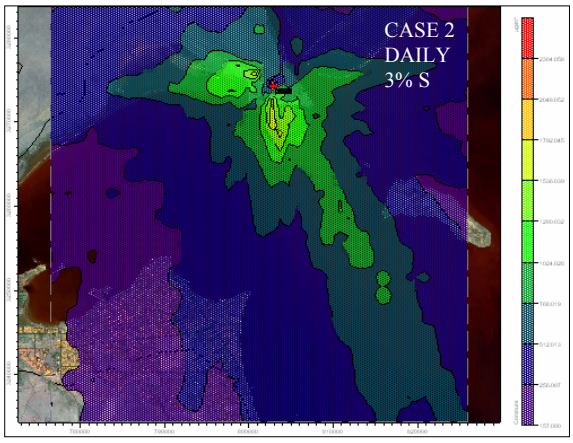

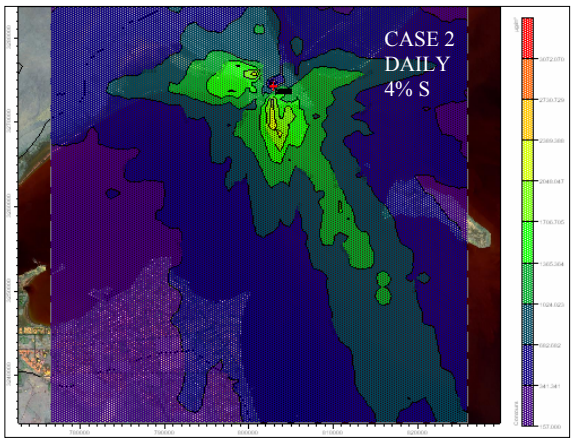

Figs. 1: Daily SO_2 concentrations due to Subiya power station for different S%

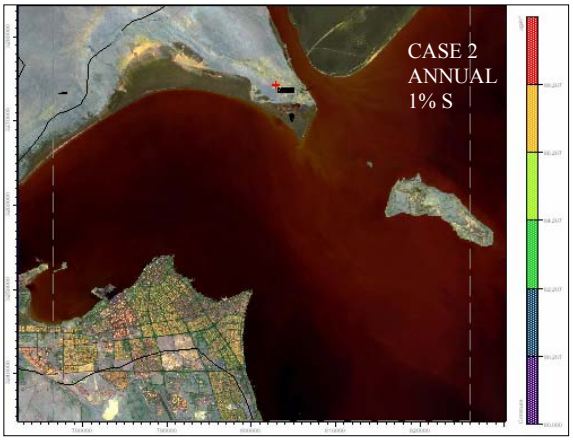

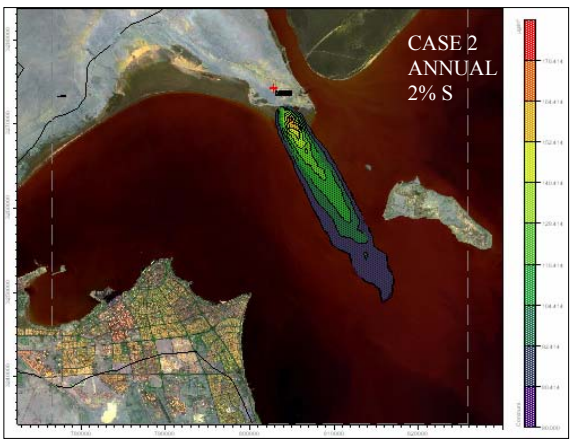

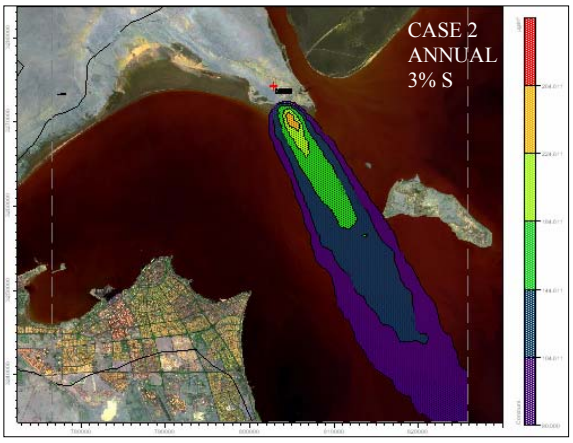

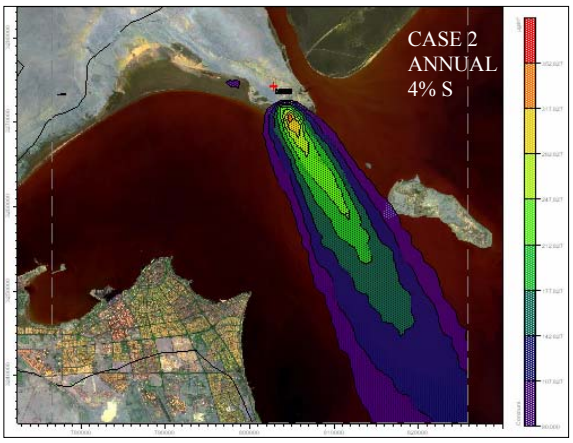

Figs. 2: Annual SO_2 concentrations due to Subiya power station for different S%

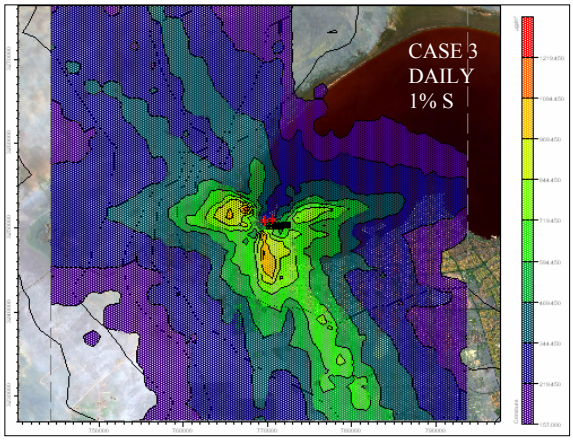

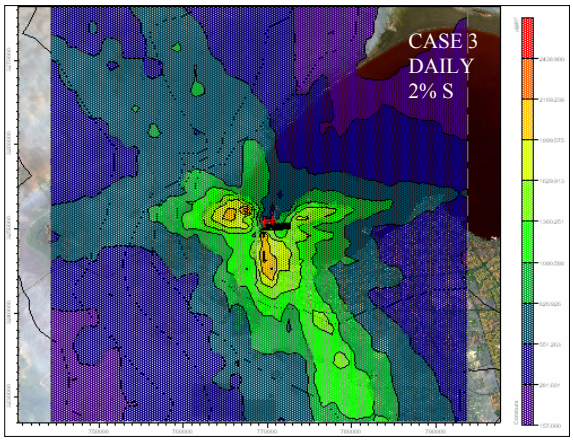

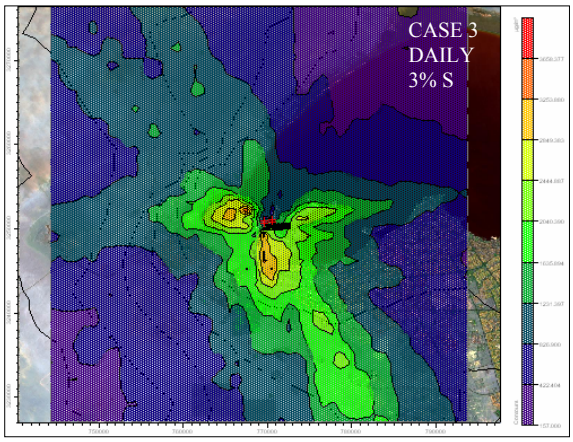

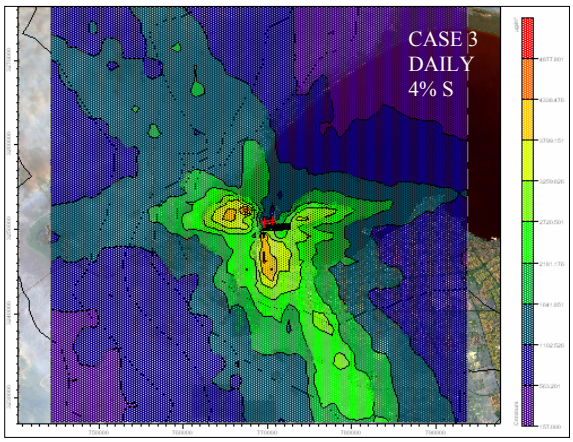

Figs. 3: Daily SO_2 concentrations due to DE and DW power station for different S%

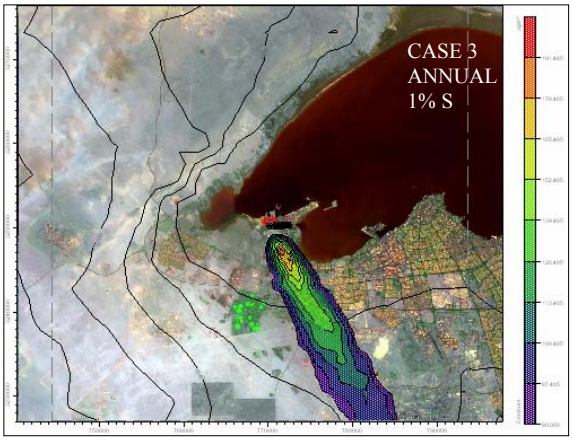

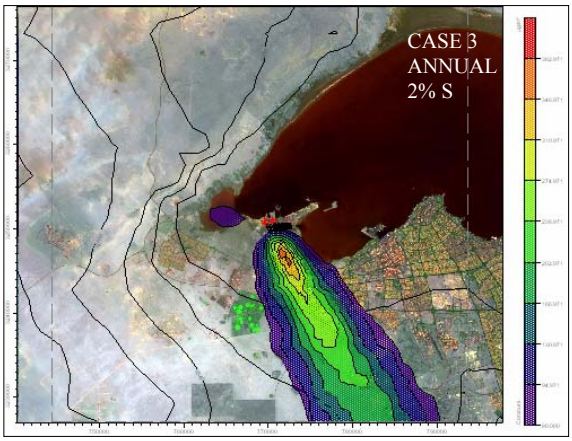

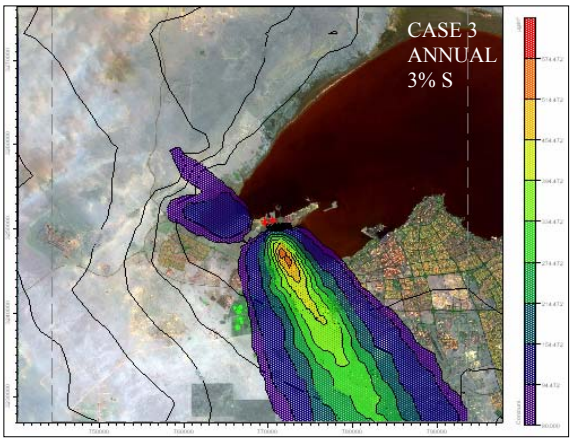

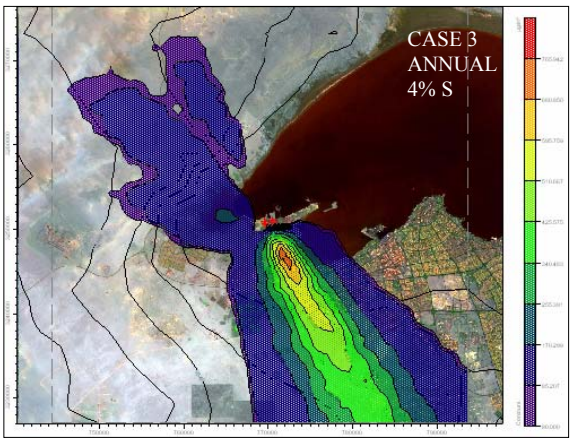

Figs. 4: Annual SO_2 concentrations due to DE and DW power station for different S%

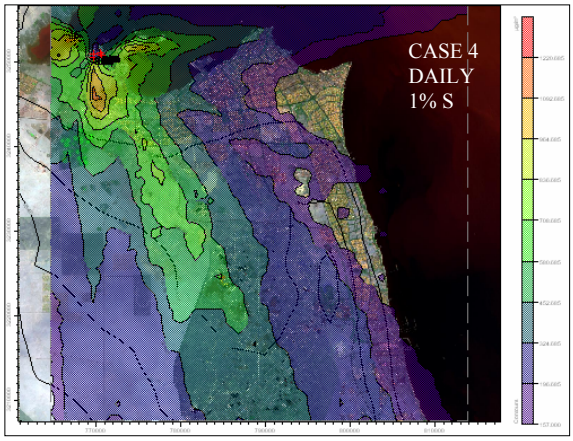

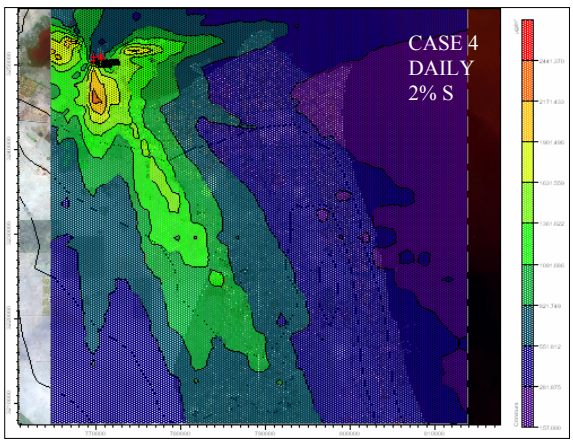

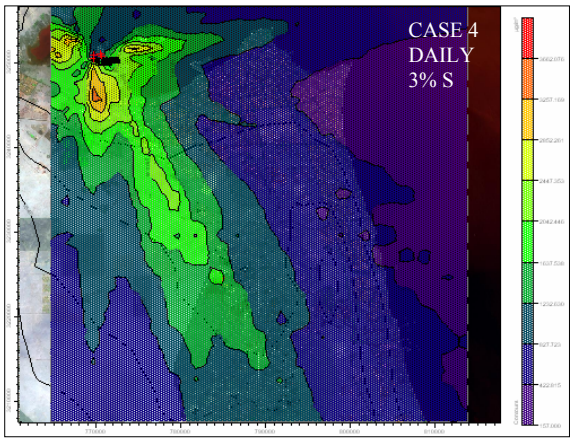

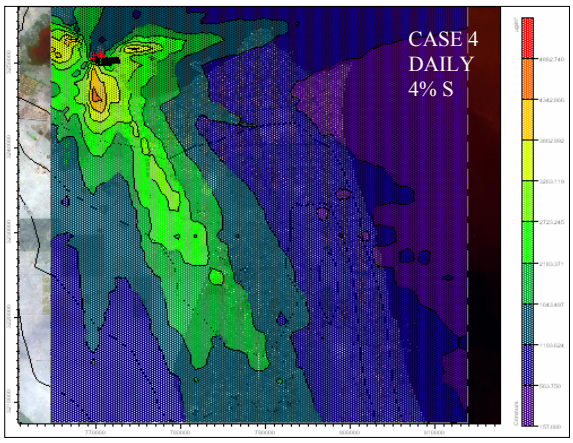

Figs. 5: Daily SO_2 concentrations due to DE and DW power station for different S% - Optimised Grid Location.

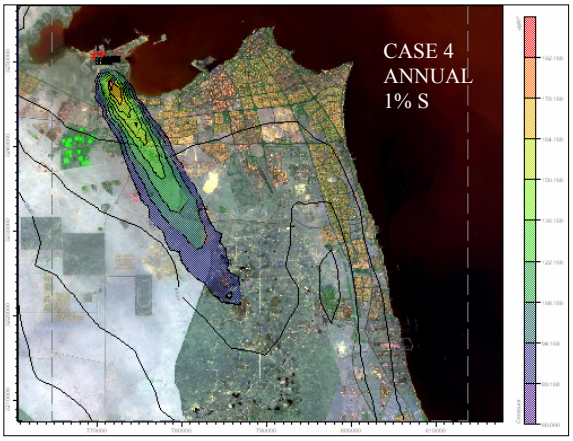

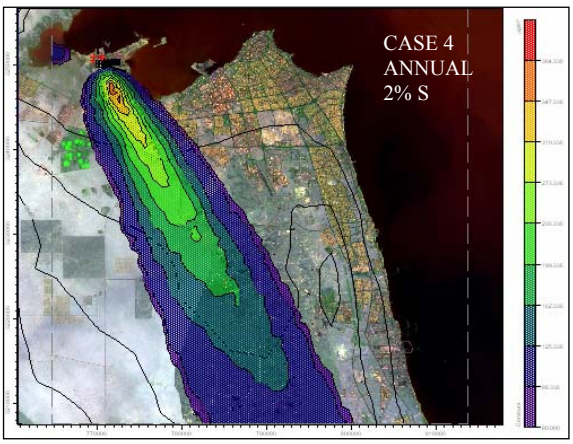

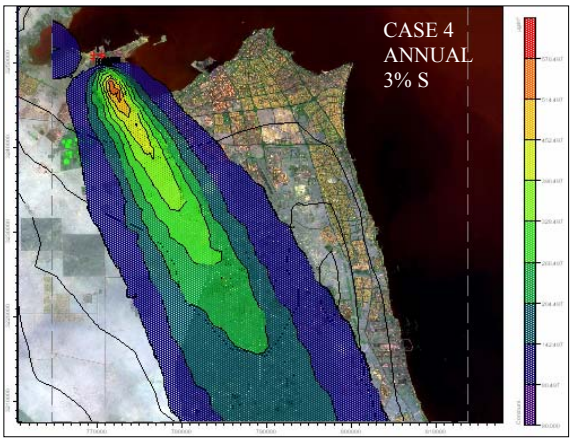

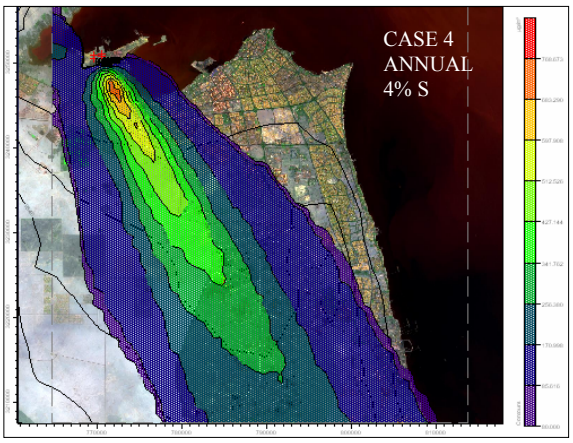

Figs. 6: Annual SO_2 concentrations due to DE and DW power station for different S% - Optimised Grid Location.